

# The novel centriolar satellite protein SSX2IP targets Cep290 to the ciliary transition zone

Maren Klinger<sup>a</sup>, Wenbo Wang<sup>a,b</sup>, Stefanie Kuhns<sup>b,\*</sup>, Felix Bärenz<sup>a,†</sup>, Stefanie Dräger-Meurer<sup>a</sup>, Gislene Pereira<sup>b</sup>, and Oliver J. Gruss<sup>a</sup>

<sup>a</sup>Zentrum für Molekulare Biologie der Universität Heidelberg and <sup>b</sup>Molecular Biology of Centrosomes and Cilia Group, Deutsches Krebsforschungszentrum–Zentrum für Molekulare Biologie der Universität Heidelberg Alliance, 69120 Heidelberg, Germany

**ABSTRACT** In differentiated human cells, primary cilia fulfill essential functions in converting mechanical or chemical stimuli into intracellular signals. Formation and maintenance of cilia require multiple functions associated with the centriole-derived basal body, from which axonemal microtubules grow and which assembles a gate to maintain the specific ciliary proteome. Here we characterize the function of a novel centriolar satellite protein, synovial sarcoma X breakpoint-interacting protein 2 (SSX2IP), in the assembly of primary cilia. We show that SSX2IP localizes to the basal body of primary cilia in human and murine ciliated cells. Using small interfering RNA knockdown in human cells, we demonstrate the importance of SSX2IP for efficient recruitment of the ciliopathy-associated satellite protein Cep290 to both satellites and the basal body. Cep290 takes a central role in gating proteins to the ciliary compartment. Consistent with that, loss of SSX2IP drastically reduces entry of the BBSome, which functions to target membrane proteins to primary cilia, and interferes with efficient accumulation of the key regulator of ciliary membrane protein targeting, Rab8. Finally, we show that SSX2IP knockdown limits targeting of the ciliary membrane protein and BBSome cargo, somatostatin receptor 3, and significantly reduces axoneme length. Our data establish SSX2IP as a novel targeting factor for ciliary membrane proteins cooperating with Cep290, the BBSome, and Rab8.

**Monitoring Editor**  
Francis A. Barr  
University of Oxford

Received: Sep 12, 2013  
Revised: Nov 6, 2013  
Accepted: Dec 12, 2013

## INTRODUCTION

Primary cilia are evolutionarily conserved organelles implicated in cellular sensory and signaling functions, which govern developmental decisions at the organismal level (Singla and Reiter, 2006; Ishikawa and Marshall, 2011). Defects in ciliogenesis lead to a wide range of

human diseases, commonly termed ciliopathies (Badano *et al.*, 2006; Fliegau *et al.*, 2007; Baker and Beales, 2009). Cilia project outward from the cell surface with their axoneme, a microtubule (MT)-based structure enclosed by the ciliary membrane. Almost all human cells form primary cilia when exiting the cell cycle and assign the older (“mother”) centriole to both nucleate axonemal MTs and serve as the basal body of the axoneme (Preble *et al.*, 2000; Kobayashi and Dynlacht, 2011). Proper ciliary functions require a compartment-specific ciliary proteome. Consistently, transitional elements radiating out from the basal body generate a diffusion barrier, which separates the ciliary membrane from the plasma membrane and the ciliary interior from the cytoplasm in order to maintain the specific ciliary proteome (Nachury *et al.*, 2010). Moreover, proteins destined for ciliary functions require specific targeting mechanisms. The prevailing model explaining targeted transport of membrane proteins to the ciliary membrane postulates that polarized exocytosis delivers proteins to the base of the cilium. The docking and fusion of exocytosed vesicles are mediated by the small GTPase Rab8 and its guanine exchange factor, Rabin 8 (Moritz *et al.*, 2001). The BBSome complex, which consists of several gene products associated with the ciliopathy

This article was published online ahead of print in MBoC in Press (<http://www.molbiolcell.org/cgi/doi/10.1091/mbc.E13-09-0526>) on December 19, 2013.

Present addresses: \*School of Biomolecular and Biomedical Science, University College Dublin, Belfield, Dublin 4, Ireland; †Deutsches Krebsforschungszentrum, In Neuenheimer Feld 280, 69120 Heidelberg, Germany.

Address correspondence to: Oliver J. Gruss ([o.gruss@zmbh.uni-heidelberg.de](mailto:o.gruss@zmbh.uni-heidelberg.de)), Gislene Pereira ([g.pereira@dkfz.de](mailto:g.pereira@dkfz.de)).

Abbreviations used: BBS, Bardet–Biedl syndrome; GFP, green fluorescent protein; IFT, intraflagellar transport; LAP, localization and affinity purification; MT, microtubule; PCM-1, pericentriolar material 1; RPE-1, retinal pigment epithelial 1; siRNA, small interfering RNA; SSTR3, somatostatin receptor 3; SSX2IP, synovial sarcoma x breakpoint 2 interacting protein.

© 2014 Klinger *et al.* This article is distributed by The American Society for Cell Biology under license from the author(s). Two months after publication it is available to the public under an Attribution–Noncommercial–Share Alike 3.0 Unported Creative Commons License (<http://creativecommons.org/licenses/by-nc-sa/3.0>).

“ASCB®,” “The American Society for Cell Biology®,” and “Molecular Biology of the Cell®” are registered trademarks of The American Society of Cell Biology.

Bardet–Biedl syndrome (BBS), directly recognizes ciliary targeting signals on ciliary membrane proteins and assembles a polymerized coat to target membrane protein clusters to the ciliary membrane. Further evidence supports the idea that BBSome–cargo complexes enter the ciliary compartment, where they interact with the intraflagellar transport (IFT; Rosenbaum and Witman, 2002) machinery at the ciliary base to be transported into the cilium (Jin *et al.*, 2010). The BBSome complex was also shown to remove non–membrane-bound proteins from the ciliary compartment (Lechtreck *et al.*, 2009, 2013).

Although the biogenesis of cilia gained much attention during the last decade, many molecular mechanisms defining ciliary protein targeting and maintenance of the ciliary compartment remain elusive. For instance, it is unclear which proteins cooperate with the BBSome in targeting ciliary membrane proteins to their final destination. Centriolar satellites are excellent candidates to mediate dynamic functions of centrosomes and basal bodies and promote targeting to basal bodies and to primary cilia. The satellites are ~70- to 100-nm proteinaceous granules, which were initially detected by electron microscopy to accumulate around centrosomes in cycling cells (Bernhard and de Harven, 1960) and surrounding basal bodies of motile cilia in epithelial cells (Sorokin, 1968; Steinman, 1968; Anderson and Brenner, 1971). A supposed key function of satellites lies in targeting centriolar and pericentriolar material from the cytoplasm to the centrosome along MTs (Kubo *et al.*, 1999; Bärenz *et al.*, 2011). Pericentriolar material protein 1 (PCM-1) is considered to be the scaffolding protein of satellites. Loss of PCM-1 leads to reduced targeting of centrin, pericentrin, and ninein to centrosomes in cycling cells (Dammermann and Merdes, 2002) and compromises primary cilia assembly (Jin *et al.*, 2010). Moreover, the satellite protein Cep290 maintains the gating functions of transitional elements at the ciliary base (Craig *et al.*, 2010; Garcia-Gonzalo *et al.*, 2011). Of interest, the BBSome subunit BBS4 is also part of centriolar satellites, implying that BBS4 may provide a molecular link between satellites and the BBSome (Nachury *et al.*, 2007).

We recently identified the synovial sarcoma X breakpoint 2–interacting protein (SSX2IP) as a novel centriolar satellite protein in cycling cells, where it acts as a maturation factor for mitotic centrosomes (Bärenz *et al.*, 2013). Here we investigate the role of SSX2IP in ciliogenesis. We show that SSX2IP interacts with the satellite protein PCM-1 and localizes to basal bodies and surrounding satellites in ciliated cells. Investigating the relationship between SSX2IP and other satellite proteins, including Cep290, Cep90, and Cep72 (Kim *et al.*, 2008; Tsang *et al.*, 2008), reveals that SSX2IP promotes the ciliary entry of the BBSome in cooperation with Cep290 but independently of Cep90 or Cep72. SSX2IP knockdown also limits the ciliary entry of both Rab8, a key regulator of ciliary targeting, and somatostatin receptor 3 (SSTR3), a membrane protein that is targeted to the cilium in a BBSome-dependent manner. Our data thus establish SSX2IP as a novel effector of primary cilia formation in human cells and reveal a new link between centriolar satellites and cilia assembly.

## RESULTS

### SSX2IP interacts and colocalizes with the centriolar satellite protein PCM-1 around basal bodies of primary cilia

We previously demonstrated that in cycling cells SSX2IP localizes to spindle poles during mitosis and can be found in centriolar satellites in interphase. Knockdown of SSX2IP causes fragmentation of the pericentriolar material in mitotic cells and defects in spindle formation accompanied by delayed alignment of metaphase chromosomes (Bärenz *et al.*, 2013). To determine the localization of SSX2IP after cell cycle exit, we tested whether SSX2IP localizes to basal

bodies of primary cilia in starved immortalized human retinal pigment epithelial (hTERT-RPE-1) cells. We determined SSX2IP localization relative to centriolar satellite proteins (PCM-1, BBS4, Cep290; Dammermann and Merdes, 2002; Kim *et al.*, 2004, 2008), centrioles (centrin; Paoletti *et al.*, 1996), the pericentriolar material ( $\gamma$ -tubulin; Zheng *et al.*, 1995), or cilia (glutamylated tubulin and IFT-88; Million *et al.*, 1999; Follit *et al.*, 2009) by indirect immunofluorescence 48 h after starvation (Figure 1a). SSX2IP localized to the basal body and showed extensive colocalization with PCM-1 (Figure 1a), suggesting that SSX2IP remains a centriolar satellite protein on basal bodies in starved cells after cell cycle exit. We confirmed localization of SSX2IP to basal bodies and centriolar satellites in murine NIH3T3 cells expressing localization and affinity purification (LAP)-tagged SSX2IP, in which the green fluorescent protein (GFP) moiety of the LAP tag allowed us to determine SSX2IP localization (Cheeseman and Desai, 2005; Figure 1b). To further investigate the relationship between SSX2IP and the satellite marker PCM-1, we performed immunoprecipitation analysis in serum-starved NIH3T3 cells stably expressing LAP-SSX2IP, using single-chain anti-GFP antibodies (GFP-binder; Rothbauer *et al.*, 2008). We quantitatively compared protein abundance in control and LAP-SSX2IP immunoprecipitates using stable isotopes to fully methylate all N-termini of tryptic peptides (dimethylation; Boersema *et al.*, 2009). This allowed us to differentiate contaminants from true LAP-SSX2IP interactors. We found PCM-1 as SSX2IP interaction partner in mass spectrometry with 6.8% sequence coverage (compared with 31.3% for SSX2IP) and high specificity (125-fold difference in abundance of sample vs. negative control, indicated by the light-to-medium ratio; Figure 1c). Specific copurification of SSX2IP and PCM-1 was confirmed by immunoblotting (Figure 1d). These data indicate that SSX2IP localizes to centriolar satellites and interacts with PCM-1 in ciliated cells.

### SSX2IP and PCM-1 localization are interdependent

To evaluate whether SSX2IP and PCM-1 are functionally related in ciliated cells, we knocked down either protein in RPE-1 cells using specific small interfering RNA (siRNA) oligonucleotides before serum starvation. Immunofluorescence and immunoblot analysis confirmed depletion of SSX2IP (Figure 2a). SSX2IP depletion did not significantly alter the overall levels of PCM-1 (Figure 2, a and b). To study possible localization changes of PCM-1 after SSX2IP knockdown, we measured the integrated density of PCM-1 signals in two areas around the centrosomal  $\gamma$ -tubulin signal: we defined a basal body region (3  $\mu\text{m}^2$  around the  $\gamma$ -tubulin spots) and a satellite region (19- $\mu\text{m}^2$  ring around the  $\gamma$ -tubulin spots; Figure 2c). Depletion of SSX2IP by two independent siRNA oligos diminished typical PCM-1 accumulation at basal bodies (Figure 2, a and d). This indicates that SSX2IP mediates efficient accumulation of PCM-1 at the basal body of ciliated cells. Next we investigated the localization of SSX2IP upon PCM-1 depletion. PCM-1 was efficiently reduced, as assessed by immunofluorescence and immunoblot analysis (Figure 2, e and f). Strikingly, knockdown of PCM-1 led to a significant decrease of the overall SSX2IP levels (Figure 2, e and f), specifically seen as reduced SSX2IP signal at basal bodies and in the satellite region (Figure 2, g and h). Taken together, these data show that PCM-1 and SSX2IP functionally interact in centriolar satellites. PCM-1 requires SSX2IP for accumulation at basal bodies, and, in turn, SSX2IP stability and basal body localization depend on PCM-1.

### Centriolar satellite proteins are differently dependent on each other

To gain further insight into the functional relationship of centriolar satellite proteins in ciliated cells, we performed SSX2IP, PCM-1,

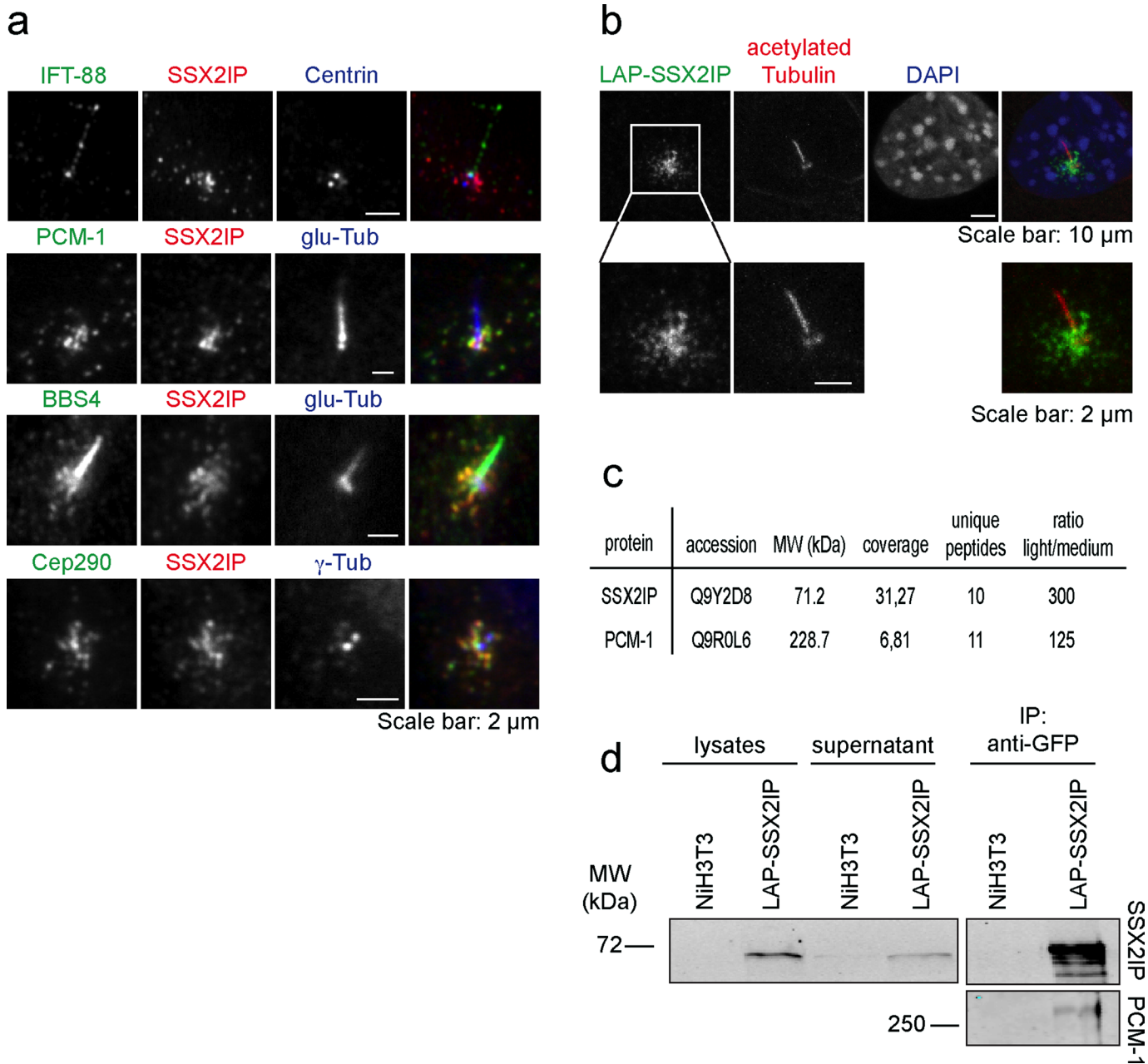
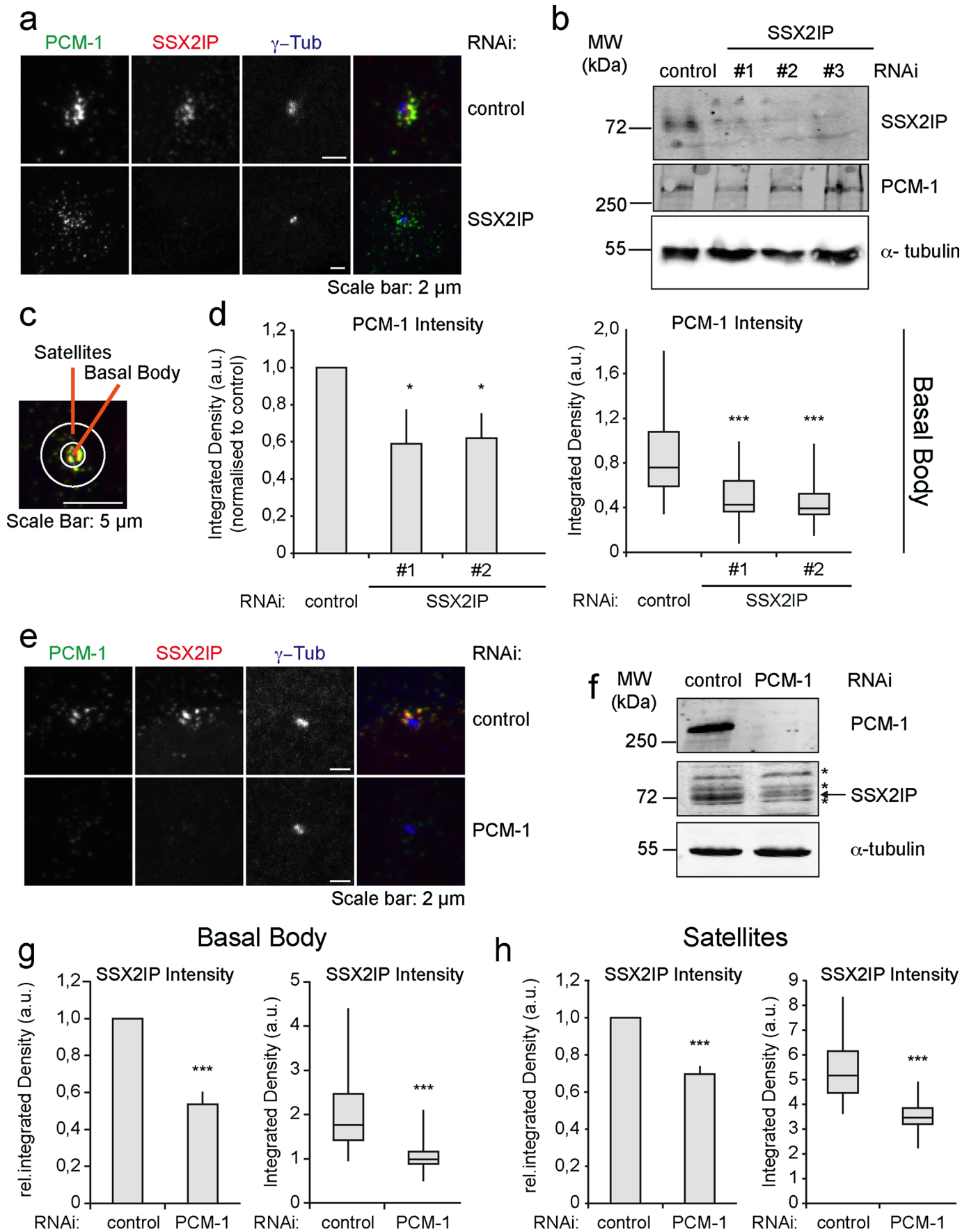


**FIGURE 1:** SSX2IP is a centriolar satellite protein localizing to basal bodies in ciliated cells. (a) Indirect immunofluorescence of serum-starved RPE-1 cells with specific antibodies as indicated; glu-tub, glutamylated tubulin. (b) Indirect immunofluorescence in NIH3T3 cells stably expressing LAP-SSX2IP (note that the LAP tag contains GFP), which was visualized with GFP antibodies. (c, d) Immunoprecipitation with single-chain GFP antibodies of lysates from serum-starved NIH3T3 cells and serum-starved NIH3T3 cells stably expressing LAP-SSX2IP. (c) Quantitative mass spectrometry analysis of immunoprecipitates. The N-termini of tryptic peptides were dimethylated using stable carbon isotopes for relative quantification of peptide abundance in SSX2IP immunoprecipitates (light) vs. control samples (medium). (d) Immunoblot shows coimmunoprecipitation of SSX2IP and PCM-1.

Cep90, or Cep290 knockdowns and studied the localization of the remaining satellite components at basal bodies and in surrounding satellites. Cep90 localizes to centriolar satellites and interacts with PCM-1 (Kim *et al.*, 2012). Its localization was not altered at basal bodies or satellites after SSX2IP knockdown (Figure 3, a, d, and h) but changed dramatically at both basal bodies and satellites after knockdown of PCM-1 (Figure 3, b, e, and i). The depletion of Cep90 (Supplemental Figure S1) reduced PCM-1 levels at basal

bodies and in the satellite region (Figure 3, c, f, and j). In contrast, SSX2IP levels in centriolar satellites remained unaffected upon Cep90 knockdown (Figure 3k) and were only slightly reduced at basal bodies (Figure 3, c and g). Therefore localization and stability of SSX2IP and Cep90 are largely independent, but both rely on PCM-1.

Next we investigated the localization of the centriolar satellite protein Cep290 after SSX2IP knockdown. It has been shown that





Cep290 interacts with PCM-1 in ciliated cells and connects axone-mal MTs to the ciliary membrane in the transition zone of *Chlamydomonas reinhardtii* (Tsang et al. 2008; Kim et al., 2008; Craige et al., 2010). Of importance, knockdown of SSX2IP in starved RPE-1 cells led to a strongly reduced Cep290 signal at basal bodies (Figure 4a). Average z-projection of 50 cells after transfection with control or SSX2IP siRNA showed loss of Cep290 from basal bodies upon SSX2IP knockdown (Figure 4b). Additional measurements revealed that Cep290 levels decreased at basal bodies and satellites (Figure 4, a, b, and d). In turn, Cep290 knockdown left SSX2IP accumulation at basal bodies and colocalization with PCM-1 unaffected (Supplemental Figure S2) and did not alter the localization of either the centriolar marker centrin or  $\gamma$ -tubulin, which served as a marker for the pericentriolar material (Supplemental Figure S3). This shows that SSX2IP ensures Cep290 accumulation at the base of primary cilia and in centriolar satellites, indicating a role of SSX2IP in targeted transport into the cilium.

### Recruitment of BBSome subunits to cilia requires SSX2IP

We next asked whether loss of SSX2IP influences targeting of the satellite component BBS4 to primary cilia (Figure 5a). On SSX2IP knockdown, only ~8% of cilia accumulated BBS4, compared with ~60% BBS4-positive cilia in controls (Figure 5b). BBS4 has a unique role among the BBSome subunits as the only subunit localizing to centriolar satellites. It was shown that release from satellites allows BBS4 to be recruited to the BBSome complex as the last subunit before ciliary targeting (Nachury et al., 2007; Zhang et al., 2012). Therefore we analyzed whether SSX2IP would also influence the recruitment of other BBSome subunits to the cilium. We first measured the ciliary levels of BBS2 (Figure 5, c and d), which cooperates with BBS7 and BBS9 to form the core complex of the BBSome (Zhang et al., 2012). Loss of SSX2IP reduced the number of BBS2-positive cilia to ~10%, compared with ~45% in controls (Figure 5d). Similarly, BBS8, which associates with the core complex together with BBS1 and BBS5 and before BBS4 incorporation (Zhang et al., 2012), did not accumulate at the basal body upon SSX2IP knockdown (Figure 5, e and f). These results clearly indicate that recruitment of the entire BBSome to the cilium depends on SSX2IP.

### Loss of SSX2IP leads to shortened cilia

The striking loss of the BBSome subunits from cilia after SSX2IP knockdown led us to reinvestigate whether SSX2IP knockdown impairs ciliogenesis in general. We transfected cells with either control or SSX2IP siRNA and visualized cilia with antibodies against glutamylated tubulin,  $\gamma$ -tubulin, and IFT-88 (Figure 6a). As a component of the IFT complex B, IFT-88 localizes along the entire axoneme, as well as to the ciliary tip (Pedersen and Rosenbaum, 2008; Schmidt et al., 2012). Loss of SSX2IP reduced the number of ciliated cells

(Figure 6b) and significantly decreased cilia length (Figure 6c), indicating that compromised targeting of ciliary proteins after SSX2IP knockdown impairs the maintenance of cilia. Of interest, knockdown of Cep290 similarly decreased the efficiency of cilia formation and reduced cilia length (Supplemental Figure S2). This further supports the idea that the primary defect in SSX2IP knockdown cells is the loss of Cep290 from the transition zone.

### SSX2IP mediates BBSome targeting through Rab8

The BBSome complex cooperates with the small GTPase Rab8 in ciliary protein targeting (Nachury et al., 2007). We therefore analyzed whether the loss of SSX2IP influences ciliary localization of Rab8. We transfected either control or SSX2IP-siRNA oligos into RPE-1 cells stably expressing Rab8-GFP and monitored Rab8 localization (Figure 7a). It is known that Rab8 enters the growing cilium together with its cargo but leaves the mature cilium. To follow cilia maturation over time, we down-regulated SSX2IP and fixed Rab8-GFP-expressing cells after different times of starvation. GFP antibodies were used to determine the localization of Rab8. Quantification of cells that contained Rab8-positive cilia revealed no SSX2IP-dependent changes in the kinetics of Rab8 entry or exit from cilia. However, loss of SSX2IP clearly interfered with the efficiency of Rab8 accumulation in cilia, leading to fewer cilia containing visible Rab8 signals at all time points after 8 h (Figure 7b). For further insights we counted Rab8-positive cells in three independent experiments after 48 h of starvation, which showed a reduction to ~40% relative to controls (Figure 7c). These results suggested that SSX2IP contributes to BBSome- and Rab8-mediated protein targeting to primary cilia.

### SSX2IP knockdown abolishes efficient accumulation of the ciliary membrane protein SSTR3

Our data demonstrated an important role for SSX2IP-dependent BBSome entry into the ciliary compartment. Together with less efficient accumulation of Rab8 during ciliogenesis, we postulated that the ciliary targeting of membrane proteins harboring a ciliary targeting signal, such as the SSTR3, may be impaired. SSTR3 belongs to the family of seven-transmembrane receptors. Coupling to adenylyl cyclase mediates somatostatin-dependent signal transduction in a variety of tissues (Pazour and Witman, 2003). Although the targeting of SSTR3 to primary cilia in RPE-1 cells was still evident (Figure 8a), SSX2IP knockdown significantly reduced the amount of SSTR3 accumulating in primary cilia (Figure 8b). In contrast, accumulation of the intraflagellar transport marker IFT88 at the tip of primary cilia (Supplemental Figure S4, a and b) was unaltered upon SSX2IP knockdown (Supplemental Figure S4c). This indicated that SSX2IP ensures efficient accumulation of ciliary membrane proteins in their compartment of destination but does not abolish ciliary trafficking in general.

**FIGURE 2:** SSX2IP stability depends on PCM-1 in RPE-1 cells. Cells were transfected with control, SSX2IP, or PCM-1 siRNA. (a) Indirect immunofluorescence detects PCM-1, SSX2IP, or  $\gamma$ -tubulin after control or SSX2IP siRNA treatment. (b) Immunoblot to document down-regulation of SSX2IP and PCM-1 after down-regulation of SSX2IP;  $\alpha$ -tubulin served as a loading control. (c) Schematic view to show the inner (basal body) area ( $3 \mu\text{m}^2$ ) and the outer (satellite) area ( $19\text{-}\mu\text{m}^2$  ring) quantified using SSX2IP (red) and PCM-1 (green) signals (d, g, h); see *Materials and Methods* for details. (d) Quantification of signal intensity of PCM-1 at the basal body after control or SSX2IP siRNA treatment. (e) Cells were transfected with control or PCM-1 siRNA and stained for PCM-1, SSX2IP, or  $\gamma$ -tubulin by indirect immunofluorescence. (f) Immunoblot to document siRNA-mediated down-regulation of PCM-1 and down-regulation of SSX2IP after PCM-1 knockdown;  $\alpha$ -tubulin served as loading control. The asterisks indicate a cross-reacting band, and the specific signal is marked by the arrow. (g, h) Quantification of signal intensities of SSX2IP at the basal body (g) and in satellites (h) after treatment with control or PCM-1 siRNA. (d, g, h) Left (bars), mean values of average intensities normalized to controls ( $\pm$ SEM) of three independent experiments ( $n \geq 150$ ). Right (box-and-whiskers plots), signal distribution of a single representative experiment. \* $p < 0.05$ , \*\* $p < 0.01$ , \*\*\* $p < 0.001$  (two-tailed Student's t test).

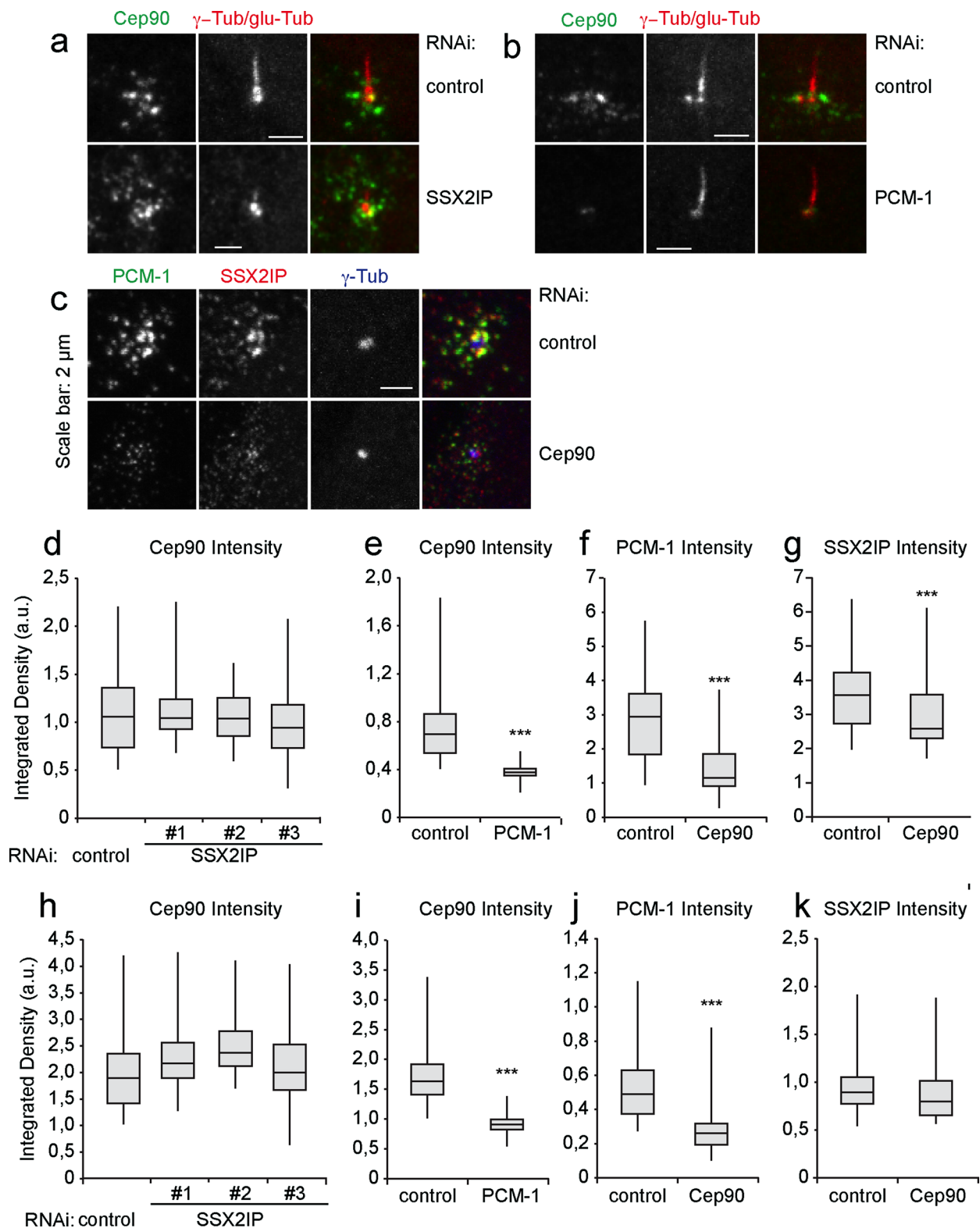


**FIGURE 3:** PCM-1 but not SSX2IP localization is dependent on Cep90 in ciliated RPE-1 cells. (a) Cells were transfected with control or SSX2IP siRNA and stained for Cep90 or  $\gamma$ -tubulin and glutamylated (glu) tubulin using indirect immunofluorescence. (b) Cells were transfected with control or PCM-1 siRNA and stained for Cep90 or  $\gamma$ -tubulin and glutamylated (glu) tubulin using indirect immunofluorescence. (c) Cells were transfected with control or Cep90s siRNA and stained for PCM-1, SSX2IP, or  $\gamma$ -tubulin using indirect immunofluorescence. (d–g) Quantification of signal intensities at basal bodies. (h–k) Quantification of signal intensities in satellites. (d, h) Cep90 signal intensity after SSX2IP knockdown. (e, i) Cep90 signal intensity after PCM-1 knockdown. (f, j) PCM-1 signal intensity after Cep90 knockdown. (g, k) SSX2IP signal intensity after Cep90 knockdown.  $n \geq 150$  from one (Cep90) or three experiments. \* $p < 0.05$ , \*\* $p < 0.01$ , \*\*\* $p < 0.001$  (two-tailed Student's *t* test).

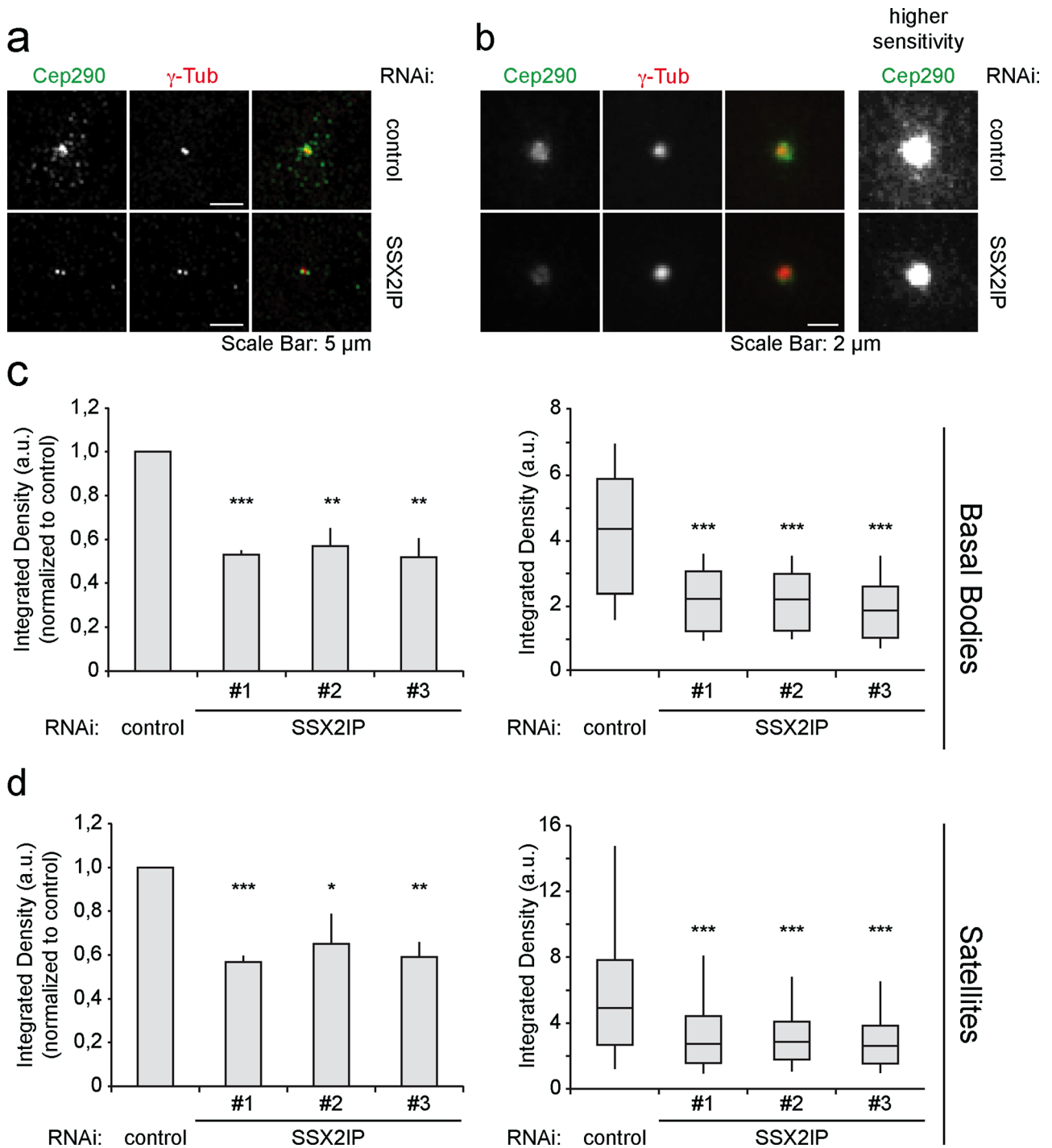


**FIGURE 4:** Cep290 recruitment to centrosomal satellites and basal bodies depends on SSX2IP in RPE-1 cells. (a) Cells were transfected with control or SSX2IP siRNA and stained for Cep290 and  $\gamma$ -tubulin using indirect immunofluorescence. (b) Average projection of 50 cells immunostained as shown in a. Centering of single images before projection was based on the  $\gamma$ -tubulin signal. (c, d) Quantification of signal intensities of Cep290 at the basal body (c) or in satellites (d) of cells transfected with control or SSX2IP siRNA. (c, d) Left (bars), mean values of averages  $\pm$  SEM from three independent experiments ( $n = 150$ ) normalized to controls. Right (box-and-whiskers plots), quantification of a single representative experiment. \* $p < 0.05$ , \*\* $p < 0.01$ , \*\*\* $p < 0.001$  (two-tailed Student's  $t$  test).

## DISCUSSION

Centriolar satellites were initially discovered as electron-dense protein granules accumulating at and near centrosomes both in cycling cells and cells that exited the cell cycle and assembled motile cilia from basal bodies (Bärenz *et al.*, 2011). The molecular composition and

function of satellites is unclear despite the identification of several satellite proteins in cells assembling primary cilia, which enabled functional analysis of single satellite proteins in cilia formation. Knockdown of PCM-1, a central scaffold for centriolar satellites, significantly reduces primary cilia formation in human cells (Nachury *et al.*, 2007),

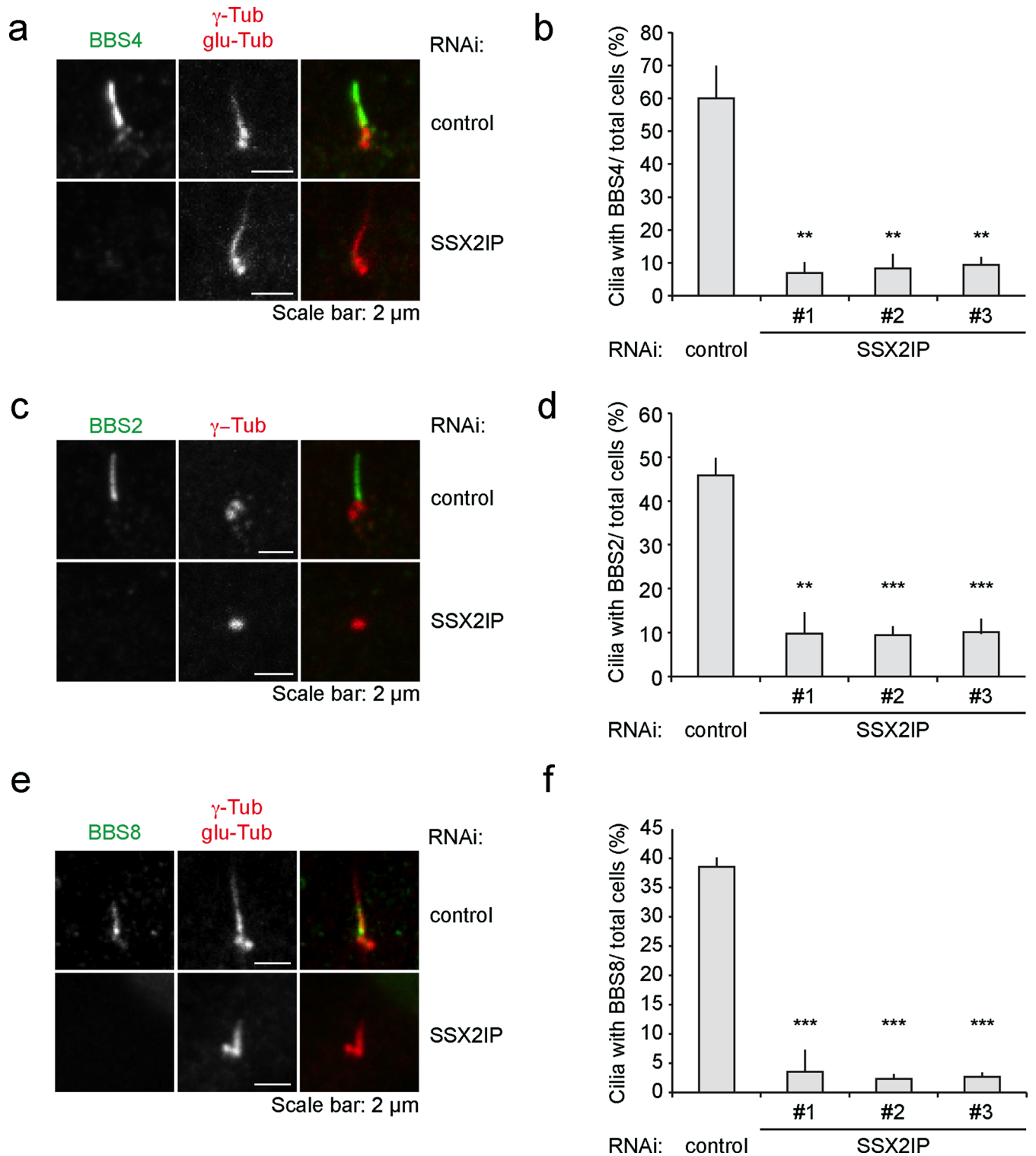


**FIGURE 5:** SSX2IP is required for ciliary BBSome localization in RPE-1 cells. (a) Cells were transfected with control or SSX2IPs siRNA and stained for BBS4 or  $\gamma$ -tubulin and glutamylated (glu) tubulin using indirect immunofluorescence. (b) Quantification of immunofluorescence shown in a. Cells with cilia showing ciliary localization of BBS4 were determined in relation to the overall cell number. (c) Cells were transfected with control or SSX2IP siRNA and stained for BBS2 or  $\gamma$ -tubulin and glutamylated (glu) tubulin using indirect immunofluorescence. (d) Quantification of immunofluorescence shown in c. Cells with cilia showing ciliary localization of BBS2 were counted in relation to the overall cell number. (e) Cells were transfected with control or SSX2IP siRNA and stained for BBS2 or  $\gamma$ -tubulin and glutamylated (glu) tubulin using indirect immunofluorescence. (f) Quantification of immunofluorescence shown in c. Cells with cilia showing ciliary localization of BBS2 were counted in relation to the overall cell number. (b, d, f) Mean values from averages from three independent experiments  $\pm$  SEM ( $n \geq 150$ ) normalized to controls. \* $p < 0.05$ , \*\* $p < 0.01$ , \*\*\* $p < 0.001$  (two-tailed Student's *t* test).



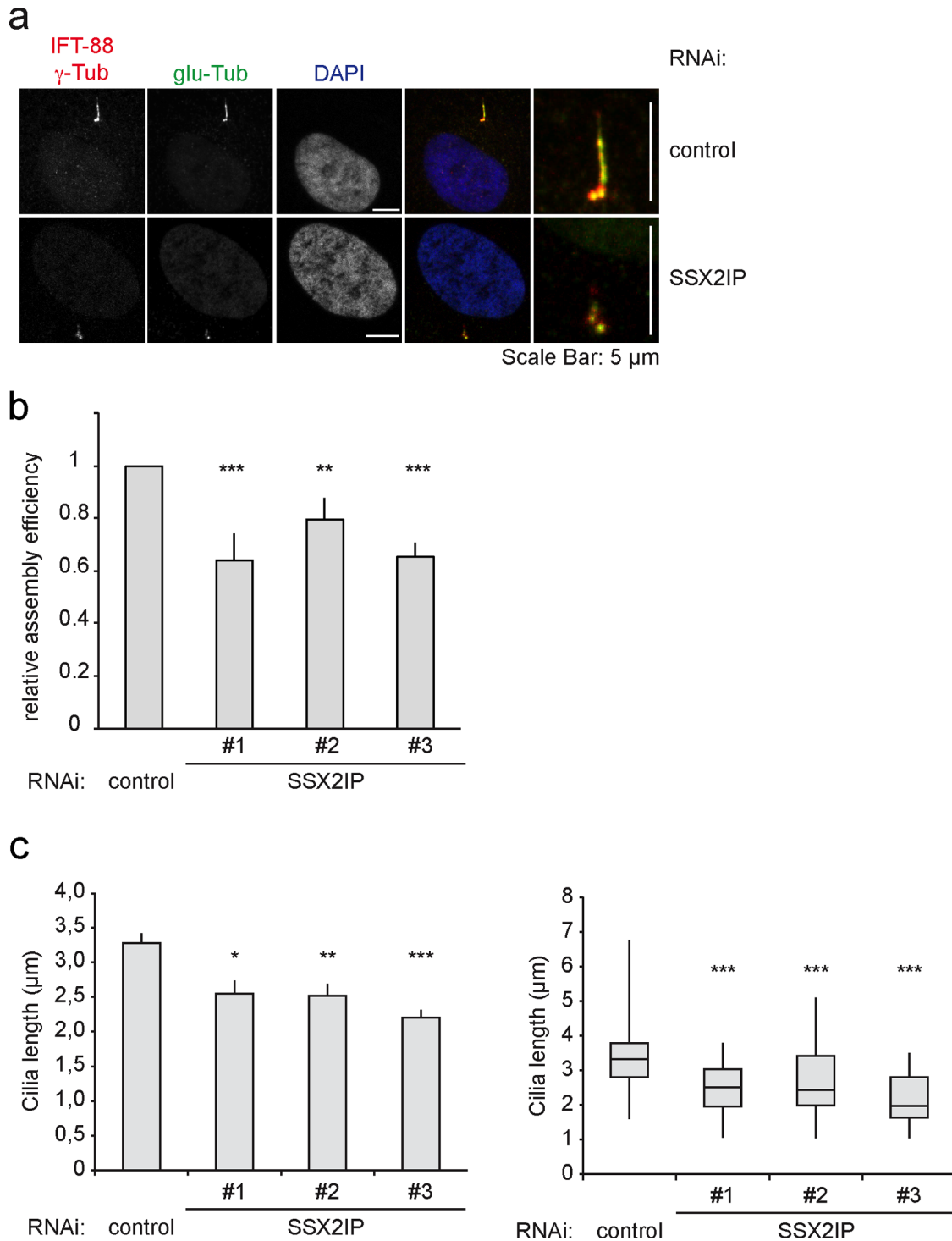


**FIGURE 6:** SSX2IP knockdown leads to less efficient ciliogenesis and shorter cilia. (a) RPE-1 cells were transfected with control or SSX2IP siRNA and stained for IFT-88,  $\gamma$ -tubulin, or glutamylated (glu) tubulin using indirect immunofluorescence. Magnified merges do not display DAPI staining. (b) Quantification of the relative cilia assembly activity in control and SSX2IP-knockdown cells. Bars show mean values  $\pm$  SEM from three independent experiments ( $n \geq 100$  cells). (c) Quantification of cilia lengths in RPE-1 cells after SSX2IP knockdown using the IFT-88,  $\gamma$ -tubulin, and glutamylated tubulin signals. Left (bars), mean values of averages  $\pm$  SEM from three independent experiments ( $n \geq 150$ ) normalized to controls. Right (box-and-whiskers plots), quantification of a single representative experiment. \* $p < 0.05$ , \*\* $p < 0.01$ , \*\*\* $p < 0.001$  (two-tailed Student's  $t$  test).

which suggests a general function of centriolar satellites in cilia assembly. BBS4 provides a direct link between satellites and cilia formation, as its recruitment from satellites to BBSomes supposedly marks the last and rate-limiting step in BBSome formation (Zhang *et al.*, 2012). It

was shown that fully assembled BBSomes enter cilia and fulfill essential functions in ciliary membrane protein targeting (Jin *et al.*, 2010).

Here we identify SSX2IP as a centriolar satellite protein, which reveals a novel twist in the role of satellites in supporting assembly

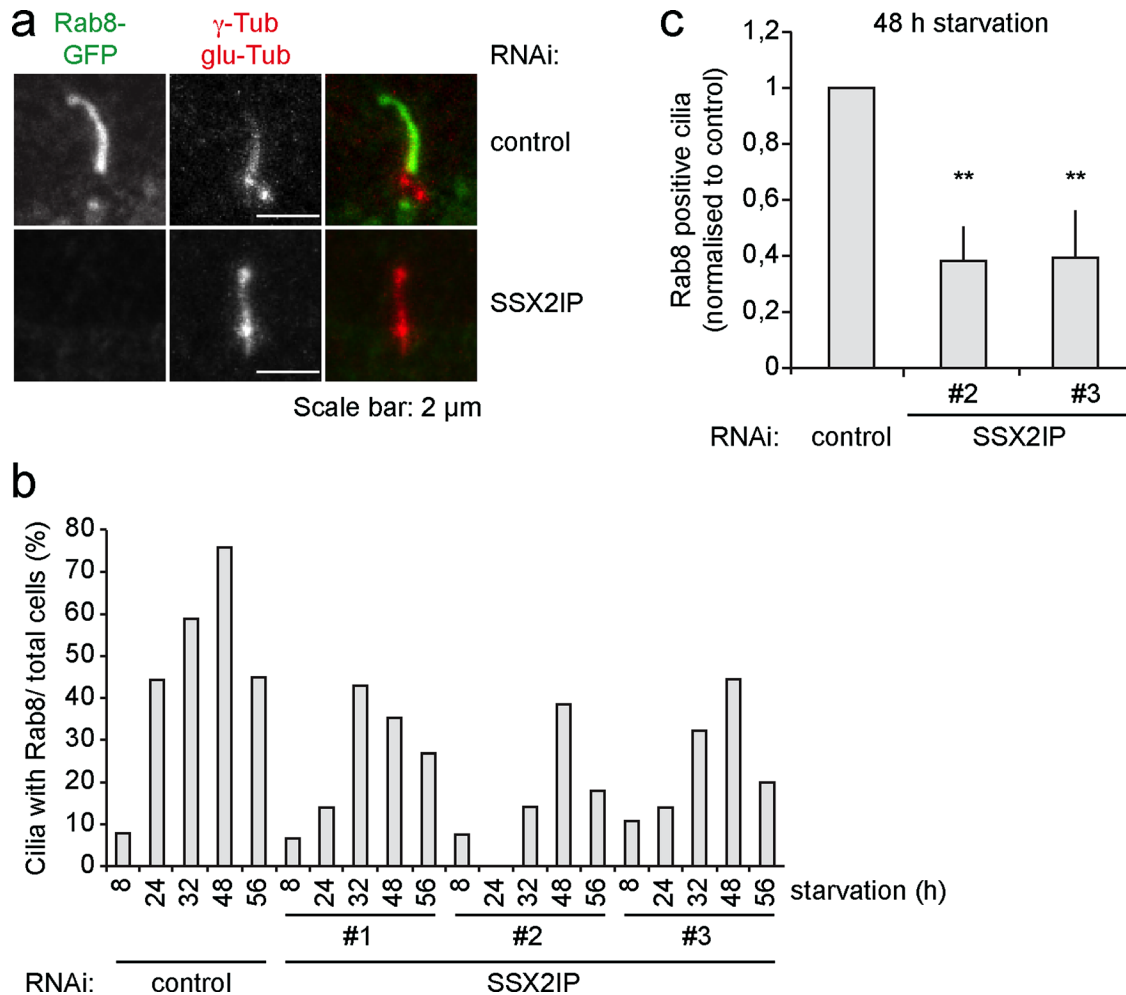


**FIGURE 7:** Ciliary accumulation of Rab8 is compromised after SSX2IP knockdown in RPE-1 cells. (a) Cells stably expressing Rab8-GFP were transfected with control or SSX2IPs siRNA and stained for GFP,  $\gamma$ -tubulin, and glutamylated (glu) tubulin using indirect immunofluorescence. (b) Quantification of immunofluorescence shown in a. Ciliated cells displaying ciliary localization of Rab8 were counted in relation to the overall cell number after different time points of serum starvation. (c) The 48-h time point of experiment shown in b. Graph shows mean values of averages ( $n \geq 150$ )  $\pm$  SEM of three independent experiments normalized to controls. \* $p < 0.05$ , \*\* $p < 0.01$ , \*\*\* $p < 0.001$  (two-tailed Student's t test).

and function of primary cilia. SSX2IP, characterized recently as a mitotic centrosome maturation factor (Bärenz *et al.*, 2013), colocalizes and interacts with PCM-1 around basal bodies of human and murine cells bearing primary cilia. Knockdown of SSX2IP completely inhibits accumulation of BBS2, BBS4, and BBS8 in the ciliary compartment. BBS2 is part of the trimeric BBSome 7/2/9 core complex, which incorporates BBS8, BBS1, and BBS5 before the recruitment of BBS4, which in turn completes BBSome assembly (Zhang *et al.*, 2012). Our data clearly indicate that targeting of the entire BBSome to the cilium requires SSX2IP. Knockdown of several recently characterized satellite proteins, including Cep90, Cep72, and the ciliopathy-associated gene product Cep290, also prevented accumulation of BBSome subunits in cilia (Kim *et al.*, 2012; Stowe *et al.*, 2012). Of interest, it was reported that BBS4 accumulates in residual cilia upon knockdown of PCM-1 (Kim *et al.*, 2012; Stowe *et al.*, 2012), indicating proper ciliary targeting of the BBSome in the absence or at low levels of PCM-1. One explanation is that loss of PCM-1 impaired the overall structure of satellites, and satellite-free BBS4 readily associated with the BBSome to enter primary cilia. In contrast, loss of the aforementioned satellite proteins from the BBSome supposedly

caused a dominant-negative situation in which satellites stayed intact but did not release BBS4 (Stowe *et al.*, 2012). In our hands, efficient PCM-1 knockdown significantly prevents BBSome entry into still-forming cilia. Consistently, PCM-1 knockdown reduces SSX2IP levels. Our data therefore question the proposal that PCM-1 prevents association of BBS4 with satellites.

Of importance, we show that the overall distribution of Cep90 is unchanged when SSX2IP levels are reduced. Our data demonstrate that Cep90 and SSX2IP have nonoverlapping functions and are independently required for BBSome accumulation in primary cilia. Moreover, knockdown of SSX2IP leads to less efficient accumulation of PCM-1 on basal bodies, whereas knockdown of Cep72 was previously shown to cause even more PCM-1 clustering around basal bodies (Stowe *et al.*, 2012). This strongly suggests that SSX2IP also functions in a parallel manner to Cep72.

Independently of Cep90 and Cep72, SSX2IP knockdown severely affects localization of Cep290 both at the basal body and in satellites, indicating that SSX2IP maintains accumulation of Cep290 both at and in the vicinity of basal bodies. Separate functions of the satellite proteins Cep90, Cep72, and SSX2IP may suggest the

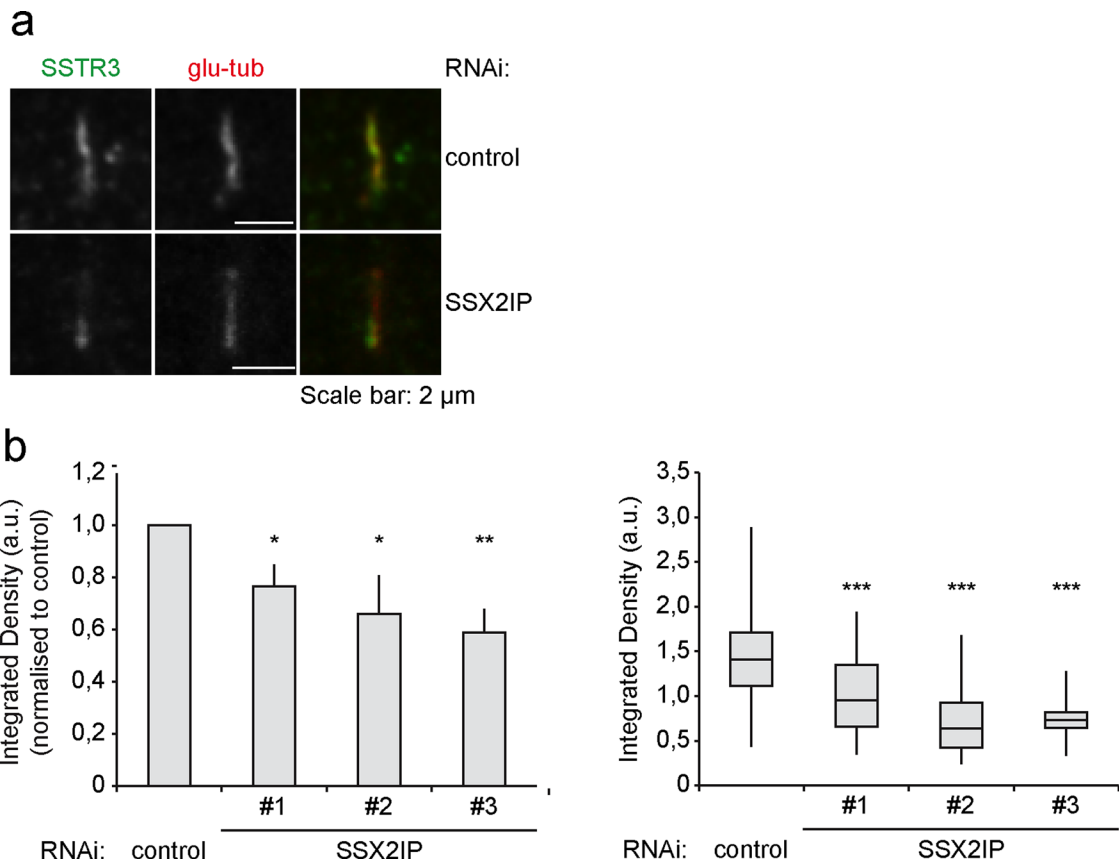


**FIGURE 8:** Transport of membrane receptor SSTR3 is impaired after SSX2IP knockdown in RPE-1 cells. (a) Cells were transfected with control or SSX2IPs siRNA and stained for SSTR3 and glutamylated (glu) tubulin using indirect immunofluorescence. (b) Quantification of signal intensity of SSTR3 in the cilium. Left (bars), mean values of averages  $\pm$  SEM from three independent experiments ( $n \geq 150$ ) normalized to controls. Right (box-and-whiskers plots), quantification of a single representative experiment. \* $p < 0.05$ , \*\* $p < 0.01$ , \*\*\* $p < 0.001$  (two-tailed Student's *t* test).

existence of different pools of centriolar satellites, the function of which could be independently required for BBSome accumulation in primary cilia. Different populations of satellites and dynamic changes of satellite composition are suggested in mitotic cells, in which SSX2IP and Cep290 lose their colocalization with PCM-1 (Lopes *et al.*, 2011; Bärenz *et al.*, 2013). Of importance, mutations in Cep290, also known as BBS14, were previously shown to correlate with several ciliopathies, including Bardet–Biedl syndrome, Meckel–Gruber syndrome, and Joubert syndrome (Staples *et al.*, 2012). This renders SSX2IP a very likely candidate for a novel ciliopathy-associated gene product.

The association with the dynein-dynactin motor complex (Bärenz *et al.*, 2013) puts SSX2IP next to BBS4, which likewise interacts with the minus end-directed MT motor and promotes PCM-1 accumulation at centrosomes (Kim *et al.*, 2004). Moreover, SSX2IP knockdown, as well as RNA interference-mediated loss of BBS4, abolished MT attachment to mitotic spindle poles and caused metaphase alignment problems in dividing cells (Kim *et al.*, 2004; Bärenz *et al.*, 2013). Both proteins may therefore also functionally interact in cycling cells.

The primary function of SSX2IP may involve its satellite and MT-binding features (Bärenz *et al.*, 2013). SSX2IP could promote dynein-dynactin-dependent transport of BBS4 itself to basal bodies. Alternatively, or in addition, SSX2IP may function to transport cargo, including Cep290, to the ciliary transition zone. The fact that loss of Cep290 diminishes ciliary accumulation of the BBSome indicates

that Cep290 promotes access of the BBSome rather than maintains a general diffusion barrier. This underlines the notion that Cep290 fulfills a gating function for proteins entering the primary cilium. Loss of this function affects the targeting of the BBSome to primary cilia.

In both cases, disturbed SSX2IP function impairs entry and accumulation of the BBSome, including BBS4, and consequently of BBSome targets, such as ciliary membrane proteins. Consistent with that, SSX2IP knockdown, as well as knockdown of Cep290 (Kim *et al.*, 2008) leads to reduced Rab8 targeting to primary cilia. Consequently, ciliary accumulation of the membrane protein SSTR3, which depends on a BBSome-recognized ciliary targeting sequence, diminished upon SSX2IP knockdown. This suggests that loss of SSX2IP changes entry of several, if not many, membrane proteins into cilia. Given that the BBSome is also involved in removing non-membrane-bound ciliary proteins from the ciliary compartment (Lechtreck *et al.*, 2009, 2013), one can speculate that SSX2IP and other centriolar satellite proteins may also mediate trafficking of soluble ciliary proteins out of the cilium. In this respect, establishing how selective loss of SSX2IP affects signaling functions of primary cilia in cells and intact organisms will constitute an important aspect of future research.

## MATERIALS AND METHODS

### Antibodies

Antibodies against human SSX2IP were produced in rabbits or guinea pigs (residues 1–438 of human SSX2IP; Bärenz *et al.*, 2013),

and human PCM-1 antibodies were generated in rabbits (residues 4993–6905 of human PCM-1; Dammermann and Merdes, 2002; Bärenz *et al.*, 2013). Antibodies against  $\gamma$ -tubulin were generated in rabbits (Zheng *et al.*, 1995; Bärenz *et al.*, 2013). Antibodies against GFP were generated in rabbits using an equimolar amount of full-length GFP and yellow fluorescent protein, produced in *Escherichia coli*. Polyclonal IFT88 antibodies were raised in rabbits as previously described (residues 365–824 of mouse IFT88; Pazour *et al.*, 2002). Mouse anti-polyglutamylated tubulin GT335 (synthetic peptide mimicking the structure of polyglutamylated sites of  $\alpha$ -tubulin) was used as an antigen (gift of C. Janke, Institut Curie, CNRS, Orsay, France; Bre *et al.*, 1994). Rabbit anti-BBS4 antibody (residues 235–519) was a kind gift from A. Fry (University of Leicester, United Kingdom). The polyclonal anti-Cep90 (rabbit) was a kind gift from Kunsoo Rhee (Seoul National University, Seoul, Korea). Antibodies from commercial sources were obtained as follows: mouse anti-acetylated tubulin (sc-23950), mouse anti-BBS2 (sc-365355), goat anti-SSTR3 (sc-11614; Santa Cruz, Heidelberg, Germany), mouse anti- $\alpha$ -tubulin (T9026), mouse anti- $\gamma$ -tubulin (T6557; Sigma-Aldrich, Taufkirchen, Germany), rabbit anti-BBS8 (HPA 003310; Sigma-Aldrich), rabbit anti-Cep290 (ab84870; Abcam, Cambridge, United Kingdom), rabbit anti-Cep131/AZ1 (A301-417A; Bethyl Laboratories, BioMol, Hamburg, Germany), and mouse anti-centrin (04-1624; EMD, Millipore, Schwalbach, Germany).

### Cell culture, transfection of siRNAs, and generation of stable SSX2IP-expressing cell line

RPE-1 cells and RPE-1 cells stably expressing Rab8-GFP (Schmidt *et al.*, 2012) were grown in DMEM/F12 (Life Technologies, Darmstadt, Germany) supplemented with 10% fetal calf serum (FCS), 2 mM L-glutamine, and 0.348% sodium bicarbonate (Life Technologies). Rab8-GFP cell lines were selected with 800  $\mu$ g/ml G418. NIH3T3 cells were grown in DMEM supplemented with 10% newborn calf serum. Transfections were performed with RNAiMAX (Life Technologies). The following siRNAs were used (all 12 nM, silencer select; Life Technologies): SSX2IP: s42130 [GGAAGGUUGC-UAUAGUGGAtt], s42131 [GCAUGUCUAAACUUACUAAAtt], and s42132 [GGGACAAUCUUUAGUGCAtt]. PCM-1: s10128 [CAAA-GACUCCACAUACGUUAtt]. Cep90: s20481 [GGCAGCUAAUUGAACGAAAtt], s20483 [CAUCGAAAGGACCAAGUAAAtt]. Cep290: s37025 [CACUUACGGACUUCGUUAAAtt], s37023 [CGUUGAUC-GACAUACUAGAtt]. After 24 h of knockdown, RPE-1 cells were incubated in serum-free medium for an additional 48 h to induce cilia formation.

Murine NIH3T3 cells lines stably expressing a fusion protein of the LAP tag (Cheeseman and Desai, 2005) fused to human SSX2IP were generated as previously described (Kuhns *et al.*, 2013).

### Pull-down experiments in stably expressing LAP-SSX2IP cells and identification of SSX2IP interaction partners by quantitative mass spectrometry

Pull downs in stably expressing LAP-SSX2IP cells were carried out as described previously (Cheeseman and Desai, 2005; Kuhns *et al.*, 2013) on immobilized GFP-nanobodies (Rothbauer *et al.*, 2008) without the second purification step on S-protein agarose. Quantitative comparison of control and SSX2IP pull-down samples was performed on all N-terminally dimethylated peptides using stable isotopes as described previously (Boersema *et al.*, 2009).

### Indirect immunofluorescence and microscopy

Cells were grown on coverslips and fixed in either ice-cold methanol for 5 min or 3% paraformaldehyde for 10 min at room

temperature. Cells were blocked with phosphate-buffered saline containing 10% FCS and 0.2% Triton X-100 for 60 min or at 4°C overnight and incubated with primary antibodies for 1 h at room temperature. Primary antibodies were detected with secondary antibodies for 60 min at room temperature. All antibodies were diluted in blocking solution. Coverslips were mounted on glass slides in Mowiol (EMD Millipore) containing 4',6-diamidino-2-phenylindole (DAPI). Images were acquired as z-stacks using the Zeiss LSM780 with a Plan-APOCHROMAT 40 $\times$ /1.3 oil immersion objective or an Olympus CellR imaging system, using a UPLSAPO 60 $\times$ /1.35 oil immersion objective.

### Fluorescence intensity measurements

Measurement of integrated density was carried out in two areas using  $\gamma$ -tubulin as a marker: basal body region (3  $\mu$ m<sup>2</sup> around the  $\gamma$ -tubulin spots) and satellite region (a 19  $\mu$ m<sup>2</sup>-ring around the  $\gamma$ -tubulin spots) using summed projections of acquired z-stacks (LSM780). From 50 to 100 cells were measured for each experimental condition. Quantification of fluorescence intensity was performed using ImageJ64 1.45S software (National Institutes of Health, Bethesda, MD).

### ACKNOWLEDGMENTS

We thank Kunsoo Rhee (Seoul National University, Seoul, Korea) for reagents. This work was supported by a Start-Professorship of the German Excellence Initiative Awarded to O.J.G.; W.W. was financed by Deutsches Krebsforschungszentrum–Zentrum für Molekulare Biologie der Universität Heidelberg Alliance Bridging Project funding granted to O.J.G. and G.P.; M.K. and W.W. are members of the Hartmut Hoffmann-Berling International Graduate School of Molecular and Cellular Biology, University of Heidelberg, Heidelberg, Germany.

### REFERENCES

- Anderson RG, Brenner RM (1971). The formation of basal bodies (centrioles) in the Rhesus monkey oviduct. *J Cell Biol* 50, 10–34.
- Badano JL, Mitsuma N, Beales PL, Katsanis N (2006). The ciliopathies: an emerging class of human genetic disorders. *Annu Rev Genomics Hum Genet* 7, 125–148.
- Bärenz F *et al.* (2013). The centriolar satellite protein SSX2IP promotes centrosome maturation. *J Cell Biol* 202, 81–95.
- Bärenz F, Mayilo D, Gruss OJ (2011). Centriolar satellites: busy orbits around the centrosome. *Eur J Cell Biol* 90, 983–989.
- Baker K, Beales PL (2009). Making sense of cilia in disease: the human ciliopathies. *Am J Med Genet C Sem Med Genet* 151C, 281–295.
- Bernhard W, de Harven E (1960). L'ultrastructure du centriole et d'autres elements de l'appareil achromatique. In: *Proceedings of the Fourth International Conference on Electron Microscopy*, Berlin: Springer-Verlag, 218–227.
- Boersema PJ, Rajmakers R, Lemeer S, Mohammed S, Heck AJ (2009). Multiplex peptide stable isotope dimethyl labeling for quantitative proteomics. *Nat Protoc* 4, 484–494.
- Bre MH, de Nechaud B, Wolff A, Fleury A (1994). Glutamylated tubulin probed in ciliates with the monoclonal antibody GT335. *Cell Motil Cytoskeleton* 27, 337–349.
- Cheeseman IM, Desai A (2005). A combined approach for the localization and tandem affinity purification of protein complexes from metazoans. *Sci STKE* 2005, pl1.
- Craige B, Tsao CC, Diener DR, Hou Y, Lechtreck KF, Rosenbaum JL, Witman GB (2010). CEP290 tethers flagellar transition zone microtubules to the membrane and regulates flagellar protein content. *J Cell Biol* 190, 927–940.
- Dammermann A, Merdes A (2002). Assembly of centrosomal proteins and microtubule organization depends on PCM-1. *J Cell Biol* 159, 255–266.
- Fliegauf M, Benzing T, Omran H (2007). When cilia go bad: cilia defects and ciliopathies. *Nat Rev Mol Cell Biol* 8, 880–893.
- Follit JA, Xu F, Keady BT, Pazour GJ (2009). Characterization of mouse IFT complex B. *Cell Motil Cytoskeleton* 66, 457–468.



- Garcia-Gonzalo FR *et al.* (2011). A transition zone complex regulates mammalian ciliogenesis and ciliary membrane composition. *Nat Genet* 43, 776–784.
- Ishikawa H, Marshall WF (2011). Ciliogenesis: building the cell's antenna. *Nat Rev Mol Cell Biol* 12, 222–234.
- Jin H, White SR, Shida T, Schulz S, Aguiar M, Gygi SP, Bazan JF, Nachury MV (2010). The conserved Bardet-Biedl syndrome proteins assemble a coat that traffics membrane proteins to cilia. *Cell* 141, 1208–1219.
- Kim JC *et al.* (2004). The Bardet-Biedl protein BBS4 targets cargo to the pericentriolar region and is required for microtubule anchoring and cell cycle progression. *Nat Genet* 36, 462–470.
- Kim J, Krishnaswami SR, Gleeson JG (2008). CEP290 interacts with the centriolar satellite component PCM-1 and is required for Rab8 localization to the primary cilium. *Hum Mol Genet* 17, 3796–3805.
- Kim K, Lee K, Rhee K (2012). CEP90 is required for the assembly and centrosomal accumulation of centriolar satellites, which is essential for primary cilia formation. *PLoS One* 7, e48196.
- Kobayashi T, Dynlacht BD (2011). Regulating the transition from centriole to basal body. *J Cell Biol* 193, 435–444.
- Kubo A, Sasaki H, Yuba-Kubo A, Tsukita S, Shiina N (1999). Centriolar satellites: molecular characterization, ATP-dependent movement toward centrioles and possible involvement in ciliogenesis. *J Cell Biol* 147, 969–980.
- Kuhns S *et al.* (2013). The microtubule affinity regulating kinase MARK4 promotes axoneme extension during early ciliogenesis. *J Cell Biol* 200, 505–522.
- Lechtreck KF, Brown JM, Sampaio JL, Craft JM, Shevchenko A, Evans JE, Witman GB (2013). Cycling of the signaling protein phospholipase D through cilia requires the BBSome only for the export phase. *J Cell Biol* 201, 249–261.
- Lechtreck KF, Johnson EC, Sakai T, Cochran D, Ballif BA, Rush J, Pazour GJ, Ikebe M, Witman GB (2009). The *Chlamydomonas reinhardtii* BBSome is an IFT cargo required for export of specific signaling proteins from flagella. *J Cell Biol* 187, 1117–1132.
- Lopes CA, Prosser SL, Romio L, Hirst RA, O'Callaghan C, Woolf AS, Fry AM (2011). Centriolar satellites are assembly points for proteins implicated in human ciliopathies, including oral-facial-digital syndrome 1. *J Cell Sci* 124, 600–612.
- Million K, Larcher J, Laoukili J, Bourguignon D, Marano F, Tournier F (1999). Polyglutamylation and polyglycylation of alpha- and beta-tubulins during in vitro ciliated cell differentiation of human respiratory epithelial cells. *J Cell Sci* 112, 4357–4366.
- Moritz OL, Tam BM, Hurd LL, Peranen J, Deretic D, Papermaster DS (2001). Mutant rab8 Impairs docking and fusion of rhodopsin-bearing post-Golgi membranes and causes cell death of transgenic *Xenopus* rods. *Mol Biol Cell* 12, 2341–2351.
- Nachury MV *et al.* (2007). A core complex of BBS proteins cooperates with the GTPase Rab8 to promote ciliary membrane biogenesis. *Cell* 129, 1201–1213.
- Nachury MV, Seeley ES, Jin H (2010). Trafficking to the ciliary membrane: how to get across the periciliary diffusion barrier. *Annu Rev Cell Dev Biol* 26, 59–87.
- Paoletti A, Moudjou M, Paintrand M, Salisbury JL, Bornens M (1996). Most of centrin in animal cells is not centrosome-associated and centrosomal centrin is confined to the distal lumen of centrioles. *J Cell Sci* 109, 3089–3102.
- Pazour GJ, Baker SA, Deane JA, Cole DG, Dickert BL, Rosenbaum JL, Witman GB, Besharse JC (2002). The intraflagellar transport protein, IFT88, is essential for vertebrate photoreceptor assembly and maintenance. *J Cell Biol* 157, 103–113.
- Pazour GJ, Witman GB (2003). The vertebrate primary cilium is a sensory organelle. *Curr Opin Cell Biol* 15, 105–110.
- Pedersen LB, Rosenbaum JL (2008). Intraflagellar transport (IFT) role in ciliary assembly, resorption and signalling. *Curr Top Dev Biol* 85, 23–61.
- Preble AM, Giddings TM Jr, Dutcher SK (2000). Basal bodies and centrioles: their function and structure. *Curr Top Dev Biol* 49, 207–233.
- Rosenbaum JL, Witman GB (2002). Intraflagellar transport. *Nat Rev Mol Cell Biol* 3, 813–825.
- Rothbauer U, Zolghadr K, Muyltermans S, Schepers A, Cardoso MC, Leonhardt H (2008). A versatile nanotrapp for biochemical and functional studies with fluorescent fusion proteins. *Mol Cell Proteomics* 7, 282–289.
- Schmidt KN, Kuhns S, Neuner A, Hub B, Zentgraf H, Pereira G (2012). Cep164 mediates vesicular docking to the mother centriole during early steps of ciliogenesis. *J Cell Biol* 199, 1083–1101.
- Singla V, Reiter JF (2006). The primary cilium as the cell's antenna: signaling at a sensory organelle. *Science* 313, 629–633.
- Sorokin SP (1968). Centriole formation and ciliogenesis. *Aspen Emphysema Conf* 11, 213–216.
- Staples CJ, Myers KN, Beveridge RD, Patil AA, Lee AJ, Swanton C, Howell M, Boulton SJ, Collis SJ (2012). The centriolar satellite protein Cep131 is important for genome stability. *J Cell Sci* 125, 4770–4779.
- Steinman RM (1968). An electron microscopic study of ciliogenesis in developing epidermis and trachea in the embryo of *Xenopus laevis*. *Am J Anat* 122, 19–55.
- Stowe TR, Wilkinson CJ, Iqbal A, Stearns T (2012). The centriolar satellite proteins Cep72 and Cep290 interact and are required for recruitment of BBS proteins to the cilium. *Mol Biol Cell* 23, 3322–3335.
- Tsang WY, Bossard C, Khanna H, Peranen J, Swaroop A, Malhotra V, Dynlacht BD (2008). CP110 suppresses primary cilia formation through its interaction with CEP290, a protein deficient in human ciliary disease. *Dev Cell* 15, 187–197.
- Zhang Q, Yu D, Seo S, Stone EM, Sheffield VC (2012). Intrinsic protein-protein interaction-mediated and chaperonin-assisted sequential assembly of stable Bardet-Biedl syndrome protein complex, the BBSome. *J Biol Chem* 287, 20625–20635.
- Zheng Y, Wong ML, Alberts B, Mitchison T (1995). Nucleation of microtubule assembly by a gamma-tubulin-containing ring complex. *Nature* 378, 578–583.